The Journal of Experimental Biology 204, 2933–2942 (2001)
Printed in Great Britain © The Company of Biologists Limited 2001
JEB3412

How the clear-sky angle of polarization pattern continues underneath clouds: full-sky measurements and implications for animal orientation

István Pomozi[1], Gábor Horváth[1,*] and Rüdiger Wehner[2]

[1]*Department of Biological Physics, Eötvös University, H-1117 Budapest, Pázmány sétány 1, Hungary,*
[2]*Institut für Zoologie, Universität Zürich, CH-8057 Zürich, Winterthurerstrasse 190, Switzerland*

*Author for correspondence (e-mail: gh@arago.elte.hu)

Accepted 8 June 2001

Summary

One of the biologically most important parameters of the cloudy sky is the proportion *P* of the celestial polarization pattern available for use in animal navigation. We evaluated this parameter by measuring the polarization patterns of clear and cloudy skies using 180° (full-sky) imaging polarimetry in the red (650 nm), green (550 nm) and blue (450 nm) ranges of the spectrum under clear and partly cloudy conditions. The resulting data were compared with the corresponding celestial polarization patterns calculated using the single-scattering Rayleigh model. We show convincingly that the pattern of the angle of polarization (e-vectors) in a clear sky continues underneath clouds if regions of the clouds and parts of the airspace between the clouds and the earth surface (being shady at the position of the observer) are directly lit by the sun. The scattering and polarization of direct sunlight on the cloud particles and in the air columns underneath the clouds result in the same e-vector pattern as that present in clear sky. This phenomenon can be exploited for animal navigation if the degree of polarization is higher than the perceptual threshold of the visual system, because the angle rather than the degree of polarization is the most important optical cue used in the polarization compass. Hence, the clouds reduce the extent of sky polarization pattern that is useful for animal orientation much less than has hitherto been assumed. We further demonstrate quantitatively that the shorter the wavelength, the greater the proportion of celestial polarization that can be used by animals under cloudy-sky conditions. As has already been suggested by others, this phenomenon may solve the ultraviolet paradox of polarization vision in insects such as hymenopterans and dipterans. The present study extends previous findings by using the technique of 180° imaging polarimetry to measure and analyse celestial polarization patterns.

Key words: polarization vision, orientation, polarization compass, skylight polarization, cloud, cloudy sky, full-sky imaging polarimetry, ultraviolet vision.

Introduction

Many animals use the sun as a compass. If the sun is not visible (hidden by clouds or vegetation or landmarks, or positioned below the horizon), several species are able to orient by means of the extensive celestial polarization pattern either in the ultraviolet or in the visible (blue or green) range of the spectrum (Wehner, 1976; Wehner, 1991). For clear skies, this pattern is quite regular and depends strongly on the celestial position of the sun. If the sky is partly clouded, its polarization pattern is rather complex because the polarization of the blue sky is disturbed by the clouds. Existing measurements of the polarization characteristics of partly clouded skies have not been carried out under wide-field conditions and, hence, are inadequate if one wishes to deduce biologically relevant information. Here, we use a 180° (full-sky) imaging polarimeter to determine the pattern of polarization of cloudy skies under clear and partly cloudy sky conditions in the visible range of the spectrum.

Many animals can infer the position of the sun from the distribution of the angle of polarization obtained from restricted regions of clear sky. Bees, for example, which often fly with most of their field of view obscured by vegetation, can orient correctly even if only spots of blue skylight are visible. Under certain conditions, skylight windows as small as 1° in diameter suffice (Edrich and von Helversen, 1976). Depending on the species, polarized light stimulating exclusively the ultraviolet, blue or green receptors located within specialized dorsal rim areas of the eye is sufficient for polarized light navigation. The required degree of polarization for successful navigation within a patch of skylight can be as low as 5–10 % (bees, Wehner, 1991; crickets, Labhart, 1996).

One of the biologically most important parameters of a cloudy sky is the proportion *P* of the celestial polarization pattern that is available to the animal's polarization compass. This parameter of clear or cloudy skies has largely been ignored in measurements of skylight polarization. Exceptions are the studies of Brines and Gould (Brines and Gould, 1982),

who made point-source measurements, and of Labhart (Labhart, 1999), who used an opto-electronic model to draw qualitative conclusions on the important role of *P* in animal orientation.

It is a well-known phenomenon that distant objects near the horizon (e.g. forests or mountains) appear blueish in colour because of Rayleigh scattering of light between the observer and these distant objects (Können, 1985; Coulson, 1988). The same phenomenon occurs in the air column underneath clouds. If part of this column is lit directly by the sun, the distribution of the angle of polarization of scattered light originating from the sunlit part of the column is the same as that of the clear sky. It is less well known that the scattering of direct sunlight on the cloud particles results in the same e-vector pattern as that of the blue sky (Können, 1985). As a result of these scattering phenomena, the angle of polarization of the sky (the most important optical cue for the animal polarization compass if the sun is not visible) underneath certain clouds approximates that of the clear sky. The celestial e-vector pattern continues underneath clouds under certain atmospheric conditions, such as when the air columns beneath clouds or parts of clouds are lit by direct sunlight: (i) obliquely from above (for smaller solar zenith angles), (ii) from the side (as with white cumuli) or (iii) from below (as sometimes occurs at dawn and dusk). The implication here is that the earth's surface has to be in sunlight, but not at the position of the observer. Below, we refer to these illumination conditions simply as 'directly lit by the sun'. Apart from heavy overcast skies with multiple cloud layers, such conditions occur frequently if the sky is partly cloudy.

Because of the lack of appropriate techniques, satisfactory measurements of the e-vector pattern in cloudy skies are not yet available. Using a point-source scanning polarimeter, Brines and Gould (Brines and Gould, 1982) measured points at every 5° elevation and azimuth angles within a half-hemisphere of the sky in 7–8 min, during which time the sun moved approximately 2° along its arc and clouds near the zenith might have been displaced considerably. Certain unavoidable errors were a consequence of their rapid measurement process, such as inaccuracies attendant upon setting the axes of the instrument. To enhance the spatial resolution of their samples by one or two orders of magnitude necessary to obtain the polarization pattern of the entire sky, their measurements would have required 70–80 min or 700–800 min, respectively, a period during which the celestial polarization pattern would change considerably as a result of the rotation of the earth (it takes 80 min for the sun to move by 20°).

The method used by Brines and Gould (Brines and Gould, 1982) – sequential measurements with a point-source scanning polarimeter – is inappropriate if the recording period is of sufficient length for the optical characteristics of the sky to change considerably. This situation will occur if the sky is cloudy, because clouds move. The displacement of clouds during such measurements will inevitably introduce so-called 'motion artefacts' to the measured values of the degree and angle of polarization of skylight, reducing their accuracy. It is clear that the polarization pattern of the whole sky cannot reliably be measured using such a time-consuming method. In contrast, an imaging polarimeter can measure reliably (without motion artefacts) the sky polarization pattern instantaneously for a huge number of celestial points, even in the presence of rapid temporal changes (e.g. displacements of clouds).

Here, we have designed and used a full-sky imaging polarimeter with which the polarization pattern of the entire sky could be measured instantaneously and accurately under diverse atmospheric conditions. Our goal was to measure and compare quantitatively the sky polarization patterns of cloudy and clear skies for different solar positions. These patterns were compared with the corresponding celestial polarization patterns calculated on the basis of the single-scattering Rayleigh model. We show firstly that the clear-sky angle of polarization pattern continues underneath clouds under certain atmospheric conditions. Secondly, we find that the shorter the wavelength in the visible range of the spectrum, the greater is the proportion of the celestial polarization pattern available underneath the clouds for animal navigation. Both results thus extend the work of Brines and Gould (Brines and Gould, 1982).

The ultraviolet-sensitivity (330–390 nm) of the polarization-sensitive area (POL area) in the dorsal eye region of hymenopterans and dipterans (Labhart and Meyer, 1999) is rather surprising because the degree of polarization of scattered skylight is generally lowest in the ultraviolet spectral region for clear skies; furthermore, the intensity of skylight is maximal in the blue range of the spectrum rather than the ultraviolet (Können, 1985; Coulson, 1988). Hence, the use of ultraviolet, the worst wavelength in this regard, is puzzling and here we term it the 'ultraviolet paradox of polarization vision'. If, however, the wavelength-dependent effect observed by us continues into the ultraviolet range of the spectrum, this phenomenon may solve the ultraviolet paradox, as suggested by Brines and Gould (Brines and Gould, 1982), although they were not able to determine quantitatively the values of *P*.

Materials and methods

Polarimetric measurements

Our clear-sky polarimetric measurements were performed in the Tunisian Chott el Djerid (33°52′ N, 8°22′ E), 10 km from Kriz, Tunisia, on 26 August 1999, when the sky was clear throughout the day. At the measurement site, sunrise and sunset was at 06:00 h and 18:55 h (local summer time = UTC+1, where UTC is universal time code), respectively. We measured the polarization pattern of the entire clear sky hourly after sunrise.

The cloudy-sky polarimetric measurements were carried out at different places and times in Tunisia from the end of August to the beginning of September 1999. From the cloudy-sky polarization patterns measured using full-sky imaging polarimetry, patterns were selected in which the solar zenith angle θ_s was approximately the same as those in the clear skies

shown in Fig. 1A–C, Fig. 2A–C. To facilitate visual comparison, the colour photographs and the patterns of the degree and angle of polarization of the cloudy sky with a given θ_s of the sun were appropriately rotated until the solar azimuth angle coincided with that in the corresponding clear sky.

Measurement of the celestial polarization pattern using full-sky imaging polarimetry

The full-sky imaging polarimetric technique used here is similar to the method of Voss and Liu (Voss and Liu, 1997). An angle of view of 180° was ensured by using a fisheye lens (Nikon-Nikkor, F=2.8, focal length 8 mm) including a built-in rotating disc mounted with three broad-band (275–750 nm) neutral density (grey) linear polarization filters (HNP′B, Polaroid Corporation, Polaroid Europe Ltd, London, UK) with three different polarization axes (0°, 45° and 90° measured from the radius of the disc). The detector was a photoemulsion in a photographic camera (Nikon F801): Fujichrome Sensia II 100 ASA colour reversal film; the maxima and half-bandwidths of its spectral sensitivity curves were λ_{red}=650±30 nm, λ_{green}=550±30 nm, λ_{blue}=450±50 nm. From a given sky, three photographs were taken for the three different alignments of the transmission axis of the polarizers on the built-in rotating disc. The camera was set up on a tripod such that its axis passing through the view-finder pointed northwards and the optical axis of the fisheye lens was vertical.

Using a personal computer, after eight-bit (true colour) digitization (using a Hewlett Packard ScanJet 6100C) and evaluation of the three developed colour pictures for a given sky, the patterns of brightness, and the degree and angle of polarization of skylight, were determined and visualized as high-resolution, colour-coded, two-dimensional circular maps. Each map contains approximately 543 000 pixels, i.e. represents approximately 543 000 measured numerical values in a given region of the spectrum. These patterns were obtained in the red, green and blue spectral ranges, in which the three colour-sensitive layers of the photoemulsion used have maximal sensitivity. The red, green and blue spectral ranges were obtained by using the scanner's digital image-processing program to separate the colour channels in the digitized images. This computerized evaluation of the three digitized photographs of a given sky is very similar to the videopolarimetry technique of Horváth and Varjú (Horváth and Varjú, 1997).

Our imaging polarimeter was calibrated as follows. The colour reversal films were all developed in the same professional photographic laboratory (in Budapest) using the same automatically controlled method. During evaluation of the recordings to obtain the brightness, degree and angle of polarization of skylight, the following characteristics of the recording and digitizing system were taken into consideration: (i) the measured Mueller matrix of the fisheye lens as a function of the angle of incidence with respect to the optical axis; (ii) the measured angular distortion of the fisheye lens *versus* the angle of incidence; (iii) the decrease in light intensity imaged on the photoemulsion because of the decrease in the effective aperture with increasing angle of incidence; (iv) the colour density curves of the colour reversal films (used as detectors) provided by the manufacturer; (v) the measured brightness and contrast transfer function of the scanner used for digitization of the colour slides of the sky. Characteristics (i-v) describe how the angular imaging, intensity, polarization and spectral composition of the incident light are influenced by the optics and detector (photoemulsion) of the polarimeter and by the scanner (digitization). Although the responses of both the photographic film and scanner were non-linear, this was taken into account, because the transfer function between the digital brightness values and the density values of the photoemulsion was measured, and the incident light intensity was calculated from this using the density-exposure characteristic curves of the film (provided by the manufacturer). Further details of the calibration of our polarimeter and the evaluation process have been published elsewhere (Gál et al., 2001).

Polarization calculations using the single-scattering Rayleigh model

The three-dimensional celestial hemisphere was represented in two dimensions by a polar-coordinate system, where the zenith angle θ and the azimuth angle φ from West are measured radially and tangentially, respectively. In this two-dimensional coordinate system, the zenith is at the origin and the horizon corresponds to the outermost circle.

The theoretical patterns of the degree and angle of polarization of skylight were calculated using the single-scattering Rayleigh model (Coulson, 1988). In the single-scattering Rayleigh atmosphere, the degree of linear polarization of skylight δ is expressed in Equation 1 and Equation 2 as:

$$\delta = \delta_{max} \sin^2\gamma/(1+\cos^2\gamma)\,, \quad (1)$$

$$\cos\gamma = \sin\theta_s \sin\theta \cos\psi + \cos\theta_s \cos\theta\,, \quad (2)$$

where γ is the angular distance between the observed celestial point and the sun, θ_s is the solar zenith angle and θ and ψ are the angular distances of the observed point from the zenith and the solar meridian, respectively. For a given θ_s, δ_{max} was determined from the patterns of the degree of polarization of skylight measured by full-sky imaging polarimetry. In the single-scattering Rayleigh atmosphere, the direction (or angle) of polarization is perpendicular to the plane of scattering determined by the observer, the celestial point observed and the sun. In the single-scattering Rayleigh model, the polarization of skylight is independent of the wavelength.

Algorithmic recognition of clouds and overexposed areas in the sky

Clouds were recognized in the digitized pictures of the sky using the following algorithm. The light intensities I_r, I_g, I_b of every pixel of the picture measured in the red, green and blue spectral ranges, respectively, were compared with each other. If the differences $\Delta I_{b-r}=|I_b-I_r|$ and $\Delta I_{b-g}=|I_b-I_g|$ were smaller than $\varepsilon=cI_b$ (where c is a constant), it was assumed that the given

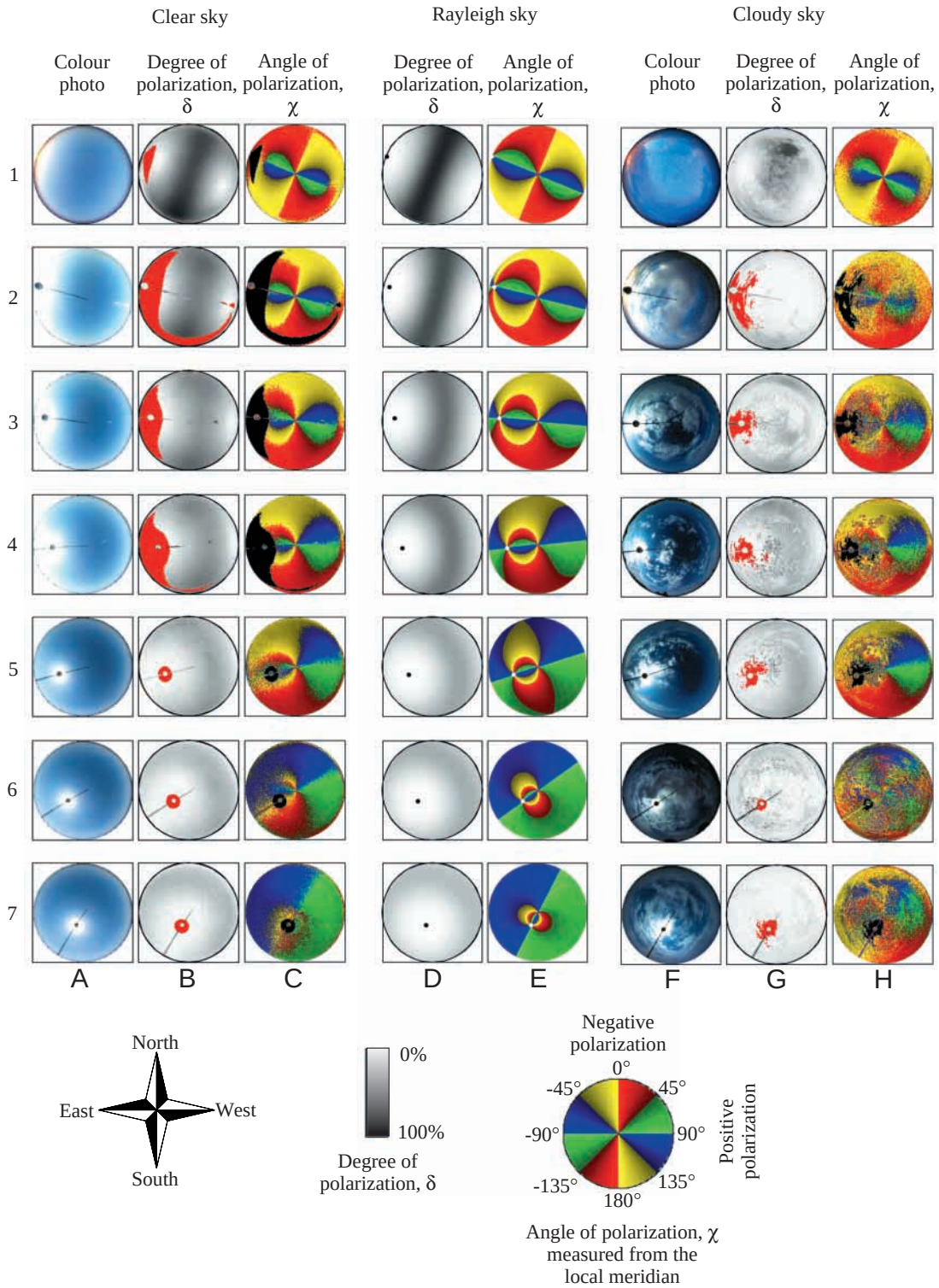

Fig. 1. (A-C) Spatial distribution of brightness and colour, degree of polarization δ and angle of polarization χ (measured from the local meridian passing through the observed celestial point) over the entire clear sky measured by full-sky imaging polarimetry in the blue (450 nm) spectral range for different hourly positions of the sun [from sunrise (06:00 h=UTC+1, where UTC is universal time code, row 1) to noon (12:00 h=UTC+1, row 7)] on 26 August 1999 in the Tunisian Chott el Djerid. (D,E) Patterns of the degree and angle of polarization of skylight calculated using the single-scattering Rayleigh model for the same positions of the sun as those in A-C. (F-H) Brightness and colour, degree of polarization and angle of polarization patterns of cloudy skies at different places in Tunisia between 27 August 1999 and 4 September 1999 measured by full-sky imaging polarimetry in the blue (450 nm) spectral range for the same solar azimuth and for approximately the same solar zenith angles as those in A–C. The red or black regions of the sky in columns B, G or C, H, respectively, are overexposed. The position of the sun is indicated by a black or white dot. The radial bar in the pictures is a wire holding a small disk to screen out the sun.

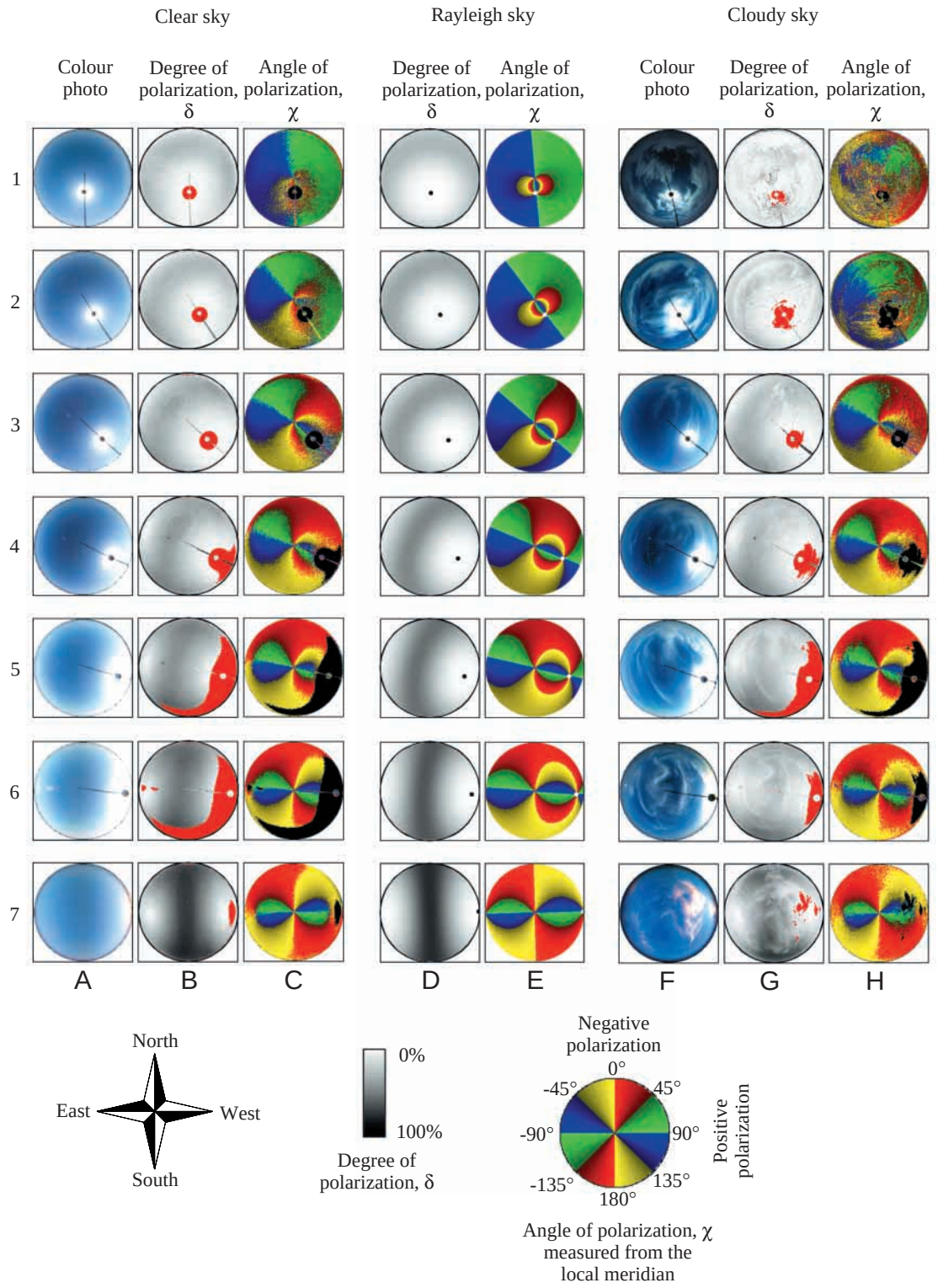

Fig. 2. As Fig. 1 from 13:00 h (=UTC+1, row 1) to 19:00 (=UTC+1, row 7, sunset).

pixel belonged to a cloud, otherwise it was attributed to the clear blue sky. The essence of this algorithm is that clouds are generally colourless (ranging from dark grey to bright white) irrespective of their brightness and position in the sky, i.e. the pixels of clouds possess approximately the same light intensities in all three (red, green, blue) spectral ranges. ε is the width of the narrow interval where the differences between I_r, I_g and I_b of a given pixel fall if the pixel is colourless enough and thus is detected as cloud. ε is proportional to the brightness I_b measured in the blue range of the spectrum because of the

blueness of scattered skylight. By setting an appropriate value of the constant *c*, we could reliably recognize clouds in the sky. Around the sun, the photoemulsion inevitably became overexposed. These colourless, white regions were recognized in the evaluation process by the same algorithm that recognized clouds.

Results

Fig. 1B,C and Fig. 2B,C represent the patterns of the degree of polarization δ and angle of polarization χ of the clear skies shown in Fig. 1A and Fig. 2A, respectively, as measured in the blue (450 nm) spectral range. The recordings were made at hourly intervals from sunrise to sunset. For comparison, Fig. 1D,E and Fig. 2D,E depict the theoretical (single-scattering Rayleigh) patterns of the degree and angle of polarization determined for the same positions of the sun as those in Fig. 1A–C and Fig. 2A–C.

Since there was no qualitative difference between the sky polarization patterns measured in the red, green and blue regions of the spectrum, we present only the celestial polarization patterns measured in the blue range of the spectrum. In general, the longer the wavelength, the higher the degree of polarization of skylight. This decrease in the degree of polarization towards shorter wavelengths is in agreement with the results of earlier point-source polarimetric measurements (Coulson, 1988) and is due mainly to the randomizing effects of multiple scattering. The degree of polarization resulting from a single scattering event is essentially independent of the wavelength. At shorter wavelengths, multiple scattering is stronger because of the stronger scattering (Rayleigh's law).

Comparison of the measured (Fig. 1B,C, Fig. 2B,C) and theoretical (Fig. 1D,E, Fig. 2D,E) patterns indicates that, apart from regions near the sun and anti-sun, the simple single-scattering Rayleigh theory describes the gross characteristics of the sky polarization patterns relatively well: (i) the degree of skylight polarization first increases with increasing angular distance from the sun, reaching its maximum at approximately 90 ° from the sun, and then decreases towards the anti-sun, and (ii) the e-vector of skylight is approximately perpendicular to the scattering plane determined by the position of the observer, the sun and the point observed.

The most striking differences between the actual and the theoretical patterns are the consequences of the neutral (unpolarized) points. We can see that, in the χ maps, the long axis of the figure-of-eight-shaped blue-green region is shorter in the actual patterns than in the Rayleigh patterns. The Arago and Babinet neutral points are positioned at the tips of this region where 'positive polarization' (direction of polarization more-or-less normal to the scattering plane, $45° < \chi \leq 135°$ with respect to the local meridian, shaded green and blue in Fig. 1C,E, Fig. 2C,E) switches to 'negative polarization' (direction of polarization more-or-less parallel to the scattering plane, $-45° \leq \chi \leq +45°$, shaded yellow and red). In the single-scattering Rayleigh model, such neutral points do not occur, or rather coincide with the anti-sun and the sun. Because of these neutral points, the isolines belonging to given values of the degree and angle of polarization differ more or less from each other in the real and the Rayleigh sky. Note, however, that since in the vicinity of these neutral points the degrees of polarization are smaller than the perceptual threshold δ_{min}=5–10 % observed in animals, the neutral points of skylight polarization are biologically irrelevant.

Fig. 1G,H and Fig. 2G,H represent the patterns of the degree and angle of polarization of cloudy skies shown in Fig. 1F and Fig. 2F, respectively, measured again in the blue (450 nm) spectral range. To ease comparison, we have chosen approximately the same solar zenith angles θ_s as those represented for clear skies in Fig. 1A–C and Fig. 2A–C. The most striking observation from Fig. 1G and Fig. 2G is that the degree of polarization is strongly reduced in those regions of the sky in which clouds appear. The clouds largely distort the normal distribution of the degree of polarization as it occurs in the clear sky. They produce discontinuities and 'holes' of very low degrees of polarization in the δ pattern of the blue sky. This observation is in accordance with previous results (Brines and Gould, 1982; Können, 1985).

However, in many cases, the patterns of the angle of polarization suffer only minor distortions when clouds are present. Compare, for example, the e-vector distributions in Fig. 1C and Fig. 2C with those in Fig. 1H and Fig. 2H. Depending on the type, thickness and height of the clouds and on the visibility of the sun (whether it is visible or hidden by clouds), the pattern of the angle of polarization that is characteristic for a clear sky largely continues underneath the clouds (e.g. Fig. 1H, rows 1–5 and Fig. 2H, rows 2–7). In certain cases, especially if the sun is close to the zenith or if it is occluded by clouds, the e-vector pattern in a cloudy sky is completely distorted (e.g. Fig. 1H, rows 6,7 and Fig. 2H, row 1).

To investigate the extent to which an insect's e-vector compass could utilise the partially disturbed e-vector patterns in cloudy skies, we should ideally feed data recorded polarimetrically from cloudy skies into the algorithmic properties of the insect's polarization-sensitive interneurons. However, the latter are not fully known. We do know from electrophysiological recordings from the polarization-sensitive (POL) interneurons in the cricket's (*Gryllus campestris*) medulla that these neurons respond reliably to e-vectors if the degree of polarization δ is greater than 5 % and that the standard deviation for the reliability of the e-vector measurements of these neurons is approximately ±6.5 ° for $5\% \leq \delta \leq 10\%$ and ±4 ° for $\delta > 10\%$ (Labhart, 1988; Labhart, 1996).

If δ is lower than the threshold value $\delta_{threshold}$=5 %, crickets cannot perceive the skylight polarization. The polarization-sensitive visual system of crickets determines the direction of the sun from the distribution of the angle of polarization of the clear sky ($\chi_{clear\ sky}$). If, in a cloudy region of the sky, the angle of polarization χ_{cloud} differs considerably from $\chi_{clear\ sky}$, the use of the χ_{cloud} value will reduce the accuracy of the

determination of the sun's direction if $\delta > \delta_{threshold}$. Crickets are not confronted with such a reduction in accuracy if the difference between $\chi_{clear\ sky}$ and χ_{cloud} is below a certain threshold $\Delta\chi_{threshold}$, which is not smaller than the reliability (±4–6.5 °) of the e-vector measurements of their POL neurons. To summarise: regions of the sky that provide reliable compass information are characterized in Equation 3 by:

$$\delta > \delta_{threshold} = 5\ \% \text{ and/or}$$
$$|\chi_{clear\ sky} - \chi_{cloud}| \leq \Delta\chi_{threshold} = 4\text{–}6.5\,^\circ . \quad (3)$$

The parameter *P* gives the proportion of the skylight pattern that can be used by the insect for reliable e-vector orientation. Fig. 3 presents two examples derived in the way described above from row 1 of Fig. 1A and F. They demonstrate that surprisingly large parts of a cloudy sky can be used by the insect for compass orientation. Increasing the value of $\delta_{threshold}$ and/or decreasing the value of $\Delta\chi_{threshold}$ will decrease *P*. Since for Fig. 3 we used $\Delta\chi_{threshold}$=6.5 ° instead of 4 °, the numerical values of *P* will be slight overestimates, at least for the vision of the cricket.

We also investigated the wavelength-dependency of the e-vector compass under cloudy conditions. Measurements were made in the blue (450 nm), green (550 nm) and red (650 nm) range of the spectrum for the clear and cloudy skies portrayed in Fig. 1A, Fig. 2A, and Fig. 1F, Fig. 2F, respectively. (i) Because of the spatial distribution of δ, the value of *P* is smaller in the solar than in the antisolar half of the celestial hemisphere. The clear-skies data (Table 1, columns A–C in Fig. 1 and Fig. 2) largely confirm what has long been deduced from atmospheric optics. (ii) The greater the amount of haze and/or aerosol concentration, the smaller is δ, and hence the smaller is *P*. (iii) In general, in clear skies, *P* is always very high (>80 %). It is influenced by the spectral content, the solar zenith angle and, of course, meteorological conditions. (iv) The lower the elevation of the sun, the larger the value of *P*. (v) In general, *P* increases with decreasing wavelength (see rows 5–7 of Fig. 1 and rows 1–4 of Fig. 2). This trend can no longer be observed for very small Δ*P* values between the blue, green and red range of the spectrum.

Most importantly, as shown in Table 2 and in columns F-H in Fig. 1 and Fig. 2, conclusions (i-v) also hold for cloudy skies. Only when the sun is not visible, i.e. if parts of the clouds and the air columns beneath them are not directly lit by sunlight, does *P* decrease. This can result from a low degree of polarization (rows 2, 6 and 7 of Fig. 1 and row 1 of Fig. 2) and/or from situations in which the e-vector pattern does not extend into the columns of air underneath the clouds (row 6 of Fig. 1 and row 1 of Fig. 2). The closer the sun to the horizon,

Table 1. *Proportion* P *(as a percentage) of the polarization pattern of the clear sky useful for navigation by crickets, evaluated from the clear-sky polarization patterns shown in Figs 1A and 2A*

	Fig. 1A			Fig. 2A		
Row	Red	Green	Blue	Red	Green	Blue
1	98.18	98.94	98.48	84.20	91.05	93.04
2	99.86	99.89	99.81	87.80	94.47	96.58
3	97.83	98.92	97.70	91.13	97.44	98.57
4	98.50	98.90	98.67	90.16	97.12	97.76
5	90.70	94.25	94.57	98.62	99.57	99.19
6	87.50	92.91	93.11	99.55	99.64	99.56
7	83.56	90.66	92.85	98.73	99.45	98.87

The degree of polarization δ>5 %.

Polarization patterns shown in Fig. 1A and Fig. 2A were measured using full-sky imaging polarimetry in the red (650 nm), green (550 nm) and blue (450 nm) spectral ranges.

Number of pixels for the entire sky=543 000.

The union of overexposed regions of skies studied in the different spectral ranges was not included.

Table 2. *Proportion* P *(as a percentage) of the polarization pattern of the clear-sky regions and the clouds useful for navigation by crickets, evaluated from the polarization patterns of cloudy skies shown in Figs 1F and 2F*

	Clear-sky regions						Clouds					
	Fig. 1F			Fig. 2F			Fig. 1F			Fig. 2F		
Row	Red	Green	Blue	Red	Green	Blue	Red	Green	Blue	Red	Green	Blue
1	95.54	93.78	77.82	77.07	79.78	83.92	47.58	59.27	62.28	4.18	4.91	16.02
2	52.82	53.85	68.35	89.81	96.56	98.09	12.93	11.09	18.42	11.72	29.51	44.23
3	90.52	93.88	95.99	90.61	95.93	97.61	27.56	32.56	42.55	43.02	51.80	63.72
4	95.13	97.41	99.28	90.78	96.64	97.42	21.81	21.35	29.42	17.01	32.89	60.69
5	94.72	97.45	97.77	95.61	98.57	98.27	19.86	21.63	24.21	61.87	71.13	81.21
6	92.92	94.63	94.10	98.15	99.72	99.76	6.76	8.32	12.89	49.48	57.05	66.83
7	71.71	76.82	86.62	98.49	98.86	98.29	3.06	2.91	9.43	36.63	58.06	71.77

For clear-sky regions, the degree of polarization δ>5 %.

For cloudy regions, δ>5 % and $|\chi_{clear\ sky}-\chi_{clouds}|\leq 6.5\,^\circ$, where χ is the angle of polarization.

Polarization patterns shown in Fig. 1F and Fig. 2F were measured using full-sky imaging polarimetry in the red (650 nm), green (550 nm) and blue (450 nm) spectral ranges.

Number of pixels for the entire sky=543 000.

The union of overexposed regions of skies studied in the different spectral ranges was not included.

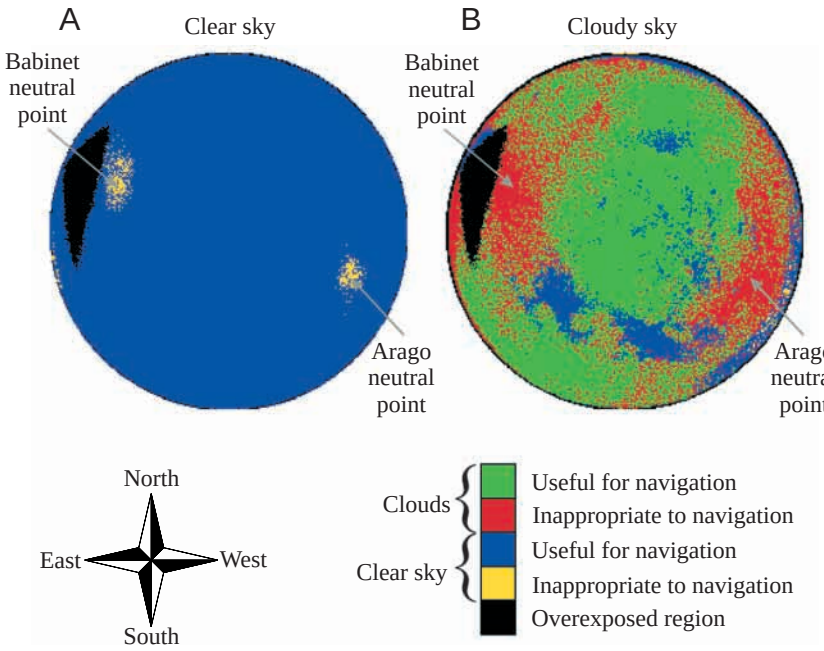

Fig. 3. Regions of the clear (A) and cloudy (B) sky shown in Fig. 1A,1 and F,1, respectively, with polarization patterns useful for or inappropriate to reliable cricket navigation calculated on the basis of the celestial polarization patterns measured by full-sky imaging polarimetry in the blue (450 nm) spectral range. Blue (useful for navigation): regions of the clear sky where the degree of polarization $\delta > 5\,\%$. Yellow (inappropriate to navigation): regions of the clear sky where $\delta \leq 5\,\%$. Green (useful for navigation): regions of the clouds where $\delta > 5\,\%$ and $|\chi_{\text{clear sky}} - \chi_{\text{clouds}}| \leq 6.5\,°$, where χ is the angle of polarization. Red (inappropriate to navigation): regions of the clouds where $\delta \leq 5\,\%$ and/or $|\chi_{\text{clear sky}} - \chi_{\text{clouds}}| > 6.5\,°$. Black: region of the sky where the photoemulsion was overexposed. The numerical values of δ, $\chi_{\text{clear sky}}$ and χ_{clouds} originate from quantitative full-sky measurements.

the larger the cloudy-sky values of *P*, because the low elevation of the sun increases the chance that the air volumes underneath clouds are directly illuminated by the sun. The shorter the wavelength, the larger the *P* values underneath the clouds. As there are no known qualitative differences between the polarization characteristics of the sky/clouds in the ultraviolet and blue spectral ranges (Können, 1985; Coulson, 1988), the latter trend, observed for the visible spectral range, can also be extrapolated to the ultraviolet range of the spectrum. These conclusions were drawn not only from the examples presented here but also from quantitative data obtained under a variety of other atmospheric conditions ranging from clear (cloudless) skies through cloudy to completely overcast skies and for solar zenith angles ranging from 15 ° to 90 °.

Discussion

Continuation of the clear-sky e-vector pattern underneath clouds

The polarization of light originating from an area of the sky covered by cloud (below termed ‘cloud light’) consists of two components. The first originates from the cloud itself. White light illuminating the cloud remains white but becomes partially linearly polarized after scattering on the cloud particles (ice crystals or water droplets). The second component is caused by the scattering of light within the air column between the cloud and the observer. This column emits blueish and linearly polarized light. Apart from very high clouds (higher than approximately 5 km), the intensity of the first component is much greater than that of the second. When the clouds and the atmosphere underneath them are directly lit by the sun (in a partly clouded sky, under thin clouds or in fog), the angle of polarization of cloud light follows the same geometrical rule as is the case in blue sky. Because of the randomizing effect of multiple scattering within clouds, the degree of polarization of the first component is usually much lower than that of the clear sky. In general, the first component dominates (its intensity is much greater than that of the second component), so the net degree of polarization of cloud light is rather low and usually reaches maximal values of approximately 40 % at 90 ° from the sun (see pp. 40–41 in Können, 1985). As there are many different types of clouds, and as the degree of polarization of cloud light depends on a multitude of factors, the degree of polarization may differ from cloud to cloud. It is usually lower for denser clouds, because of the randomizing effect of diffuse scattering by the cloud particles.

In contrast to ice-clouds, water-clouds are strongly polarized not only at 90 ° but also at approximately 145 ° from the sun, where the degree of polarization can reach 60 %, i.e. potentially higher values than in the background skylight (see pp. 42–43 in Können, 1985). At 145 ° from the sun, water-clouds are markedly brighter than at other regions in the sky.

If the clouds are not thin and/or parts of them are not directly illuminated by the sun, their polarization characteristics differ from those discussed above. Under a heavily overcast sky, when the cloud layer is several kilometres thick, the illumination comes more or less from all directions and, hence, the degree of polarization of the clouds is strongly reduced (see pp. 42–43 in Können, 1985). More light will come from the zenith, where the clouds look thinnest, than from the horizon, meaning that the cloud light will be horizontally polarized. The degree of polarization of this cloud light reaches maximal values of 10–20 % just above the horizon and decreases rapidly towards the zenith, where it is 0 %. A similar polarization pattern occurs in fog not illuminated by direct sunlight. When

the clouds are very thick and the visibility is poor (e.g. during rain), the illumination is extremely diffuse, so that the degree of skylight polarization is reduced to zero.

Our full-sky imaging polarimetric measurements show that, even though in cloudy skies the degree of polarization may differ markedly from that in a cloudless sky, the angle of polarization does not. Consider, for example, rows 2–7 in Fig. 2H: the majority of the sky was covered by thin strato-cumulus and stratus clouds, which considerably reduced the degree of polarization, but the pattern of the angles of polarization remained identical to that in the corresponding clear skies (rows 2–7 in Fig. 2C). In rows 1–5 of Fig. 1H thicker and lower clouds were present, which totally distorted the degree of celestial polarization, but left the e-vector patterns underneath the clouds (Fig. 1C, rows 1–5) unaltered because parts of the clouds were illuminated directly by sunlight. In contrast, in rows 6 and 7 of Fig. 1H and row 1 of Fig. 2H the patterns of both the degree and angle of polarization were quite different from those of clear skies (Fig. 1C, rows 6,7 and Fig. 2C, row 1), because the sun was hidden by thicker clouds and the clouds were not directly lit by the sun.

On the basis of the physiological properties of polarization-sensitive interneurons recorded by Labhart (Labhart, 1996), we can compute the proportion of the celestial e-vector pattern, that even under cloudy skies, can be exploited for navigation (if compared with the full e-vector pattern under clear-sky conditions). Under all but the most extreme cloud-cover conditions, this proportion is rather large. Hence, clouds decrease the extent of skylight polarization useful for animal orientation much less than hitherto assumed.

Ultraviolet paradox of polarization vision

More than a quarter of a century ago, it was discovered that desert ants *Cataglyphis bicolor* (Duelli and Wehner, 1973) and honey bees *Apis mellifera* (von Helversen and Edrich, 1974) use ultraviolet receptors in a specialized dorsal rim area of the eye (Wehner, 1982; Wehner and Strasser, 1985) as polarization analyzers. It was subsequently found that, in other groups of insects, blue and green rather than ultraviolet receptors are used as polarization analyzers (for a review, see Labhart and Meyer, 1999). Why is there such diversity and why should ultraviolet receptors be favoured by long-distance navigators such as bees and ants? This appears surprising because, in scattered light, the degree of polarization is lowest in the ultraviolet range of the spectrum (Coulson, 1988; Horváth and Wehner, 1999).

von Frisch (von Frisch, 1965) assumed that the pattern of polarized light is most stable in the ultraviolet region, but there is no theoretical basis for this assumption. Mazokhin-Porshnyakov (Mazokhin-Porshnyakov, 1969) suggested that, by using the ultraviolet spectral range, insects ensured that they used polarized light in the sky rather than polarized reflections from the ground, which are richer in long-wavelength radiation. As we now know, however, it is only a tiny area of the eye of the ant or bee that is sensitive to polarized light, and this area is oriented towards the sky, so that the ambiguities envisaged by Mazokhin-Porshnyakov (Mazokhin-Porshnyakov, 1969) are unlikely to arise. In a theoretical approach, Seliger et al. (Seliger et al., 1994) surmised that polarization-sensitive photopigments that are most efficient under conditions of a high degree of skylight polarization should have their maximum sensitivity λ_{max} at 450 nm, whereas ultraviolet photopigments (λ_{max}=350 nm) would maximize the signal-to-noise ratio under low degrees of polarization. Finally, Brines and Gould (Brines and Gould, 1982) suggested that polarization vision might have evolved during geological times when the earth's atmosphere absorbed less ultraviolet radiation than it does today. They further assumed that ultraviolet receptors might have some advantages over long-wavelength receptors under certain atmospheric conditions such as cloudy skies. Wehner (Wehner, 1994) has given a detailed description of why e-vector patterns under clouds should be more reliable in the ultraviolet. In our present account, we find that the extension of the e-vector pattern of the blue sky into the areas of the sky covered by clouds is more useful to an e-vector compass when the observer responds to shorter wavelengths, as suggested by Brines and Gould (Brines and Gould, 1982).

This work was supported by a three-year János Bolyai postdoctoral research fellowship to G.H. from the Hungarian Academy of Sciences. The grants OTKA F-025826 to G.H. from the Hungarian National Science Foundation and 31-43317.95 to R.W. from the Swiss National Science Foundation are gratefully acknowledged. Thanks are due to an anonymous referee for his valuable comments.

References

Brines, M. L. and Gould, J. L. (1982). Skylight polarization patterns and animal orientation. *J. Exp. Biol.* **96**, 69–91.

Coulson, K. L. (1988). *Polarization and Intensity of Light in the Atmosphere*. Hampton, VA: A. Deepak Publishing.

Duelli, P. and Wehner, R. (1973). The spectral sensitivity of polarized light orientation in *Cataglyphis bicolor* (Formicidae, Hymenoptera). *J. Comp. Physiol.* **86**, 37–53.

Edrich, W. and von Helversen, O. (1976). Polarized light orientation of the honey bee: the minimum visual angle. *J. Comp. Physiol.* **109**, 309–314.

von Frisch, K. (1965). *Tanzsprache und Orientierung der Bienen.* Berlin: Springer.

Gál, J., Horváth, G., Meyer-Rochow, V. B. and Wehner, R. (2001). Polarization patterns of the summer sky and its neutral points measured by full-sky imaging polarimetry in Finnish Lapland north of the Arctic Circle. *Proc. R. Soc. Lond. A* **457**, 1385–1399.

von Helversen, O. and Edrich, W. (1974). Der Polarisationsempfänger im Bienenauge: ein Ultraviolettrezepor. *J. Comp. Physiol.* **94**, 33–47.

Horváth, G. and Varjú, D. (1997). Polarization pattern of freshwater habitats recorded by video polarimetry in red, green and blue spectral ranges and its relevance for water detection by aquatic insects. *J. Exp. Biol.* **200**, 1155–1163.

Horváth, G. and Wehner, R. (1999). Skylight polarization as perceived by desert ants and measured by video polarimetry. *J. Comp. Physiol. A* **184**, 1–7 [Erratum **184**, 347–349 (1999)].

Können, G. P. (1985). *Polarized Light in Nature*. Cambridge: Cambridge University Press.

Labhart, T. (1988). Polarization-opponent interneurons in the insect visual system. *Nature* **331**, 435–437.

Labhart, T. (1996). How polarization-sensitive interneurones of crickets perform at low degrees of polarization. *J. Exp. Biol.* **199**, 1467–1475.

Labhart, T. (1999). How polarization-sensitive interneurones of crickets see the polarization pattern of the sky: a field study with an opto-electronic model neurone. *J. Exp. Biol.* **202**, 757–770.

Labhart, T. and Meyer, E. P. (1999). Detectors for polarized skylight in insects: a survey of ommatidial specializations in the dorsal rim area of the compound eye. *Microsc. Res. Technol.* **47**, 368–379.

Mazokhin-Porshnyakov, G. A. (1969). *Insect Vision*. New York: Plenum Press.

Seliger, H. H., Lall, A. B. and Biggley, W. H. (1994). Blue through UV polarization sensitivities in insects: optimizations for the range of atmospheric polarization conditions. *J. Comp. Physiol. A* **175**, 475–486.

Voss, K. J. and Liu, Y. (1997). Polarized radiance distribution measurements of skylight. I. System description and characterization. *Appl. Opt.* **36**, 6083–6094.

Wehner, R. (1976). Polarized-light navigation by insects. *Sci. Am.* **235**, 106–115.

Wehner, R. (1982). Himmelsnavigation bei Insekten. Neurophysiologie und Verhalten. *Neujahrsbl. Naturforsch. Ges. Zürich* **184**, 1–132.

Wehner, R. and Strasser, S. (1985). The POL area of the honey bee's eye: behavioural evidence. *Physiol. Ent.* **10**, 337–349.

Wehner, R. (1991). Visuelle Navigation: Kleinsthirn-Strategien. *Verh. Dt. Zool. Ges.* **84**, 89–104.

Wehner, R. (1994). The polarization-vision project: championing organismic biology. In *Neural Basis of Behavioural Adaptation* (ed. K. Schildberger and N. Elsner), pp. 103–143. Stuttgart, New York: G. Fischer.